

Smart Grids Volt-VAR Frequency Control: A Smart Building Distributed Model Predictive Control Based Approach

S.Masoom Maroufi
Department of Electrical Engineering
University of Bologna
Bologna, Italy
seyede.maroufi@studio.unibo.it

Raul V. A. Monteiro
Department of Electrical Engineering
Federal University of Mato Grosso
Cuiaba, MT, Brazil
raulvitor@ufmt.br

Arturo Bretas, Surya C. Dhulipala
Department of Electrical and Computer Engineering
University of Florida
Gainesville, FL
arturo@ece.ufl.edu, chandandhulipala@ufl.edu

Abstract—High penetration levels of in Distributed Energy Resources (DERs) as low-inertia renewable energy sources into smart grids imposes imperative Volt-VAR Control (VVC) as well as stability challenges for Distribution Network (DN) operation. Although numerous approaches harness traditional VVC devices to compensate for voltage violations, synthetic inertia and control of energy storage systems exist to improve transient stability with an increase of DERs. While ample strategies tackle these two problems separately, the ability of smart buildings to provide active and reactive power support simultaneously to the grid has not yet been fully exploited. In this work, the effect of the modulation of loads' apparent power consumption on the grid's frequency and voltage profile have been explored. A Distributed Model Predictive Control (DMPC) strategy is presented for voltage and frequency control in the DN provided by smart buildings. The robustness of this strategy is validated on a modified IEEE 13 bus system.

Index Terms—Distribution networks; frequency control; model predictive control; smart buildings; thermostatically controlled loads; voltage control.

I. INTRODUCTION

Power systems controls aim to maintain system voltages, frequency, and other system variables within their acceptable limits. These limits are to be respected when of normal load and generation variations as well as large disturbances [1].

Load dynamics result in voltage variation. To keep the voltage in the desired range, equipment distributed through out the system are used in the traditional Volt/VAR control. Traditional Volt/VAR control consider load tap changing transformers, shunt reactors for long distance Extra High Voltage (EHV) and Ultra High Voltage (UHV) transmission lines, and shunt capacitors to maintain the desired voltage profile by injecting the reactive power into the line [2], [3].

Although the traditional reactive power compensation methods have helped to mitigate the negative effects of voltage regulation on the grid, many studies suggest that they cannot

attenuate the detriments of high renewable power source penetration. As the current reactive power compensation techniques cannot alleviate power quality problems due to the larger impact of renewable sources, there is a need for VAR control on a faster time scale [4].

Imbalances between load and generation must be corrected within seconds as well to avoid frequency deviations that might threaten the stability and security of the power system [5]. The conventional method of correcting frequency deviation is focused on primary frequency responses. In this way, the deviation between demand and generation is corrected by adjusting the generation outputs [6]. As is the case with conventional voltage correction techniques, this method suffers from high latency in adapting to low-inertia, renewable power source penetration.

As many buildings have control systems to monitor and adjust their power consumption, [7], [8], [9], and [10] have explored the use of Heating, Ventilation, and Air Conditioning (HVAC) units and other Thermostatically Controlled Loads (TCLs) to provide frequency regulation services to the grid. While [11] shows that HVAC systems in commercial buildings can provide demand side system frequency regulation, [12] illustrates how one can use smart buildings for Volt/VAR control.

As [12] focuses only Volt-Var problem, it fails to address frequency regulation. In this work we extend [12] aiming to provide additional auxiliary grid services, specifically simultaneous distribution networks voltage and frequency control obtained through smart buildings active power consumption modulation. Smart buildings which allow apparent power modulation are considered. Local Quality of Service, (QoS), established using Distributed Model Predictive Control (DMPC), and the global QoS are simultaneously considered.

This paper is organized into six sections. In Section II,

the state-space model for HVAC systems and the DMPC strategy are presented. In Section III, the reactive and active power estimation model considering local measurements and sensitivity analysis is derived. In Section IV, determination of apparent power is formulated as a cost minimization problem. Simulation results, discussion, and analysis are presented in Section V. Finally, conclusions and future work are discussed in Section VI.

II. MODELING & CONTROL STRATEGY

A. HVAC State Space Model

For the estimation of the thermal loads, the Equivalent Thermal Parameter (ETP) modeling approach is used. As this method is presented thoroughly in [13], only the mathematical models used for the state space description of ETP are presented, as follows:

$$\dot{x} = Ax + Bu, \quad y = Cx + Du \quad (1)$$

$$\dot{x} = \begin{bmatrix} \dot{T}_{air} \\ \dot{T}_{mass} \end{bmatrix}, \quad x = \begin{bmatrix} T_{air} \\ T_{mass} \end{bmatrix}, \quad u = 1 \quad (2)$$

$$A = \begin{bmatrix} -\left(\frac{1}{R_2 \cdot C_{air}} + \frac{1}{R_1 \cdot C_{air}}\right) & \frac{1}{R_1 \cdot C_{air}} \\ \frac{1}{R_2 \cdot C_{mass}} & -\left(\frac{1}{R_2 \cdot C_{air}}\right) \end{bmatrix} \quad (3)$$

$$B = \begin{bmatrix} \frac{T_0}{R_1 \cdot C_{air}} + \frac{Q}{C_{air}} \\ 0 \end{bmatrix}$$

$$C = \begin{bmatrix} 1 & 0 \\ 0 & 1 \end{bmatrix}, \quad D = \begin{bmatrix} 0 \\ 0 \end{bmatrix}. \quad (4)$$

Where:

$$R_1 = 1/UA_{insul}$$

$$R_2 = 1/UA_{mass}$$

$$C_{air} = \text{air heat capacity (Btu/}^\circ\text{C)}$$

$$C_{mass} = \text{mass (building and contents) heat capacity(Btu/}^\circ\text{C)}$$

$$UA_{insul} = \text{the heat gain/loss coefficient (Btu/}^\circ\text{C)}$$

$$UA_{mass} = \text{the heat gain/loss coefficient between air and mass (Btu/}^\circ\text{C)}$$

$$T_{air} = \text{air temperature inside the building (}^\circ\text{C)}$$

$$T_{mass} = \text{mass temperature inside the building (}^\circ\text{C)}$$

B. Control Strategy

In [12], a Model Predictive Control (MPC) approach is used as the control strategy for the Volt-VAR problem. The step-by-step procedure of deriving the optimized control signal for the MPC is presented in [14].

By denoting the variation of the state variable in the future $x_m(t+1)$, control variable $u(t)$, and process output $y(t)$, the triple (A,B,C) are referred to as the augmented model. The augmented model is defined based on the A_m , B_m , and C_m which depend on the plant characteristics. The state-space model can be obtained:

$$\begin{aligned} \overbrace{\begin{bmatrix} x(t+1) \\ \Delta x_m(t+1) \\ y(t+1) \end{bmatrix}}^{\text{A}} &= \overbrace{\begin{bmatrix} A_m & O_m^T \\ C_m A_m & 1 \end{bmatrix}}^{\text{A}} \overbrace{\begin{bmatrix} x(t) \\ \Delta x_m(t) \\ y(t) \end{bmatrix}}^{\text{B}} + \overbrace{\begin{bmatrix} B_m \\ C_m B_m \end{bmatrix}}^{\text{B}} \Delta u(t) \\ y(t) &= \overbrace{\begin{bmatrix} O_m & 1 \end{bmatrix}}^{\text{C}} \overbrace{\begin{bmatrix} \Delta x_m(t) \\ y(t) \end{bmatrix}}^{\text{C}} \end{aligned} \quad (5)$$

$$\text{where } O_m = \overbrace{\begin{bmatrix} 0 & 0 & \cdots & 0 \end{bmatrix}}^{n_1}.$$

The cost function J is based on our goal of adjusting the predictive control vector to have the minimum difference between Y as the predicted system trajectory vector and Y_{ref} as the reference trajectory vector. It is defined as follows:

$$\begin{aligned} \min J &= (Y_{ref} - Y)^T (Y_{ref} - Y) + \Delta U^T Q \Delta U \\ \text{Subject to } x(t+1) &= Ax(t) + Bu(t) \\ y(t) &= Cx(t) \end{aligned} \quad (6)$$

With ΔU being the predicted input vector variation and $Q = R_w I$ (I is the identity matrix $N_c \times N_c$ and R_w is the weight) being the MPC weight vector, we derive J from ΔU at each time instant for a prediction horizon N_p to have the optimal control signal that minimizes the cost function in (6). For N_c as an optimal control sequence whose first value is applied to the system in the next time instant, the solution of (6) is:

$$\Delta U = (\Phi^T \Phi + Q)^{-1} \Phi^T (Y_{ref} - Fx(t_i)). \quad (7)$$

Where F and ϕ are matrices based on the augmented model as following:

$$F = \begin{bmatrix} CA \\ CA^2 \\ \vdots \\ CA^{N_p} \end{bmatrix} \quad (8)$$

$$\Phi = \begin{bmatrix} CB & 0 & \cdots & 0 \\ CAB & CB & \cdots & 0 \\ \vdots & & & \\ CA^{N_p-1}B & CA^{N_p-2}B & \cdots & CA^{N_p-N_c}B \end{bmatrix}. \quad (9)$$

III. SENSITIVITY ANALYSIS, REACTIVE & ACTIVE POWER MODEL

For deriving the reactive and active power estimation model, the sensitivity of the system with voltage and frequency must be analysed to obtain the efficient coordination between the agents.

A. Sensitivity Analysis

The Newton-Raphson power flow technique is used to estimate system states considering bus voltage magnitudes and angles. The minimization between the functions ΔP , ΔQ , and a predefined convergence tolerance is of interest.

$$\begin{bmatrix} \Delta P \\ \Delta Q \end{bmatrix} = \begin{bmatrix} P^{exp} \\ Q^{exp} \end{bmatrix} - \begin{bmatrix} P \\ Q \end{bmatrix}. \quad (10)$$

The linearized equations obtained by the Newton-Raphson approach linearizing (10) at each time step are as follows:

$$J \begin{bmatrix} \Delta \theta \\ \Delta V \end{bmatrix} = \begin{bmatrix} \Delta P \\ \Delta Q \end{bmatrix} \quad (11)$$

$J = \begin{bmatrix} \frac{\partial P}{\partial \theta} & \frac{\partial P}{\partial V} \\ \frac{\partial Q}{\partial \theta} & \frac{\partial Q}{\partial V} \end{bmatrix}$ is the Jacobian matrix.

With a non-singular and invertible Jacobian as in [15], we can write:

$$\begin{bmatrix} \Delta \theta \\ \Delta V \end{bmatrix} = \begin{bmatrix} S_{\theta \Delta P} & S_{\theta \Delta Q} \\ S_{V \Delta P} & S_{V \Delta Q} \end{bmatrix} \begin{bmatrix} \Delta P \\ \Delta Q \end{bmatrix}. \quad (12)$$

Where:

$S_{\theta \Delta P}$ and $S_{\theta \Delta Q}$ are sensitivities of the bus voltage angles to active and reactive power;

$S_{V \Delta P}$ and $S_{V \Delta Q}$ are sensitivities of the bus voltage magnitudes to active and reactive power.

B. Reactive Power

The process of deriving reactive power from the sensitivity matrix is demonstrated with details in [12]. For i being the bus providing reactive power and j being the bus which voltage regulation is desired, we present the predicted Q at time $t+1$ based on Q at time t by assuming $S_{v \Delta P_{ij}} = 0$:

$$Q_{t+1} = Q_t + \frac{V_{Reference} - V_{measurement}}{S_{v \Delta Q_{ij}}}. \quad (13)$$

C. Active Power

We use the same model to estimate the active power bus i provides to maintain the desired voltage angle, θ , at bus j

$$\Delta \theta_j = S_{\theta \Delta P_{ij}} \Delta P_i + S_{\theta \Delta Q_{ij}} \Delta Q_i \quad (14)$$

$$\theta_{reference} - \theta_{measurement} = S_{\theta \Delta P_{ij}} \Delta P_i + S_{\theta \Delta Q_{ij}} \Delta Q_i \quad (15)$$

$$P_{t+1} = P_t + \frac{(\theta_{reference} - \theta_{measurement}) - S_{\theta \Delta Q_{ij}} \Delta Q_i}{S_{\theta \Delta P_{ij}}}. \quad (16)$$

Assuming $S_{\theta \Delta Q_{ij}} = 0$:

$$\theta_{reference} - \theta_{measurement} = S_{\theta \Delta P_{ij}} \Delta P_i. \quad (17)$$

Same as Q , here we predict P at $t+1$ with the current P , reference angle, and measured angle:

$$P_{t+1} = P_t + \frac{\theta_{Reference} - \theta_{measurement}}{S_{v \Delta P_{ij}}} \quad (18)$$

by assuming $C_{ij}(\Delta P_{ij})$, the cost incurred to supply P_{ij} active power to improve voltage at bus 'j' by bus 'i' we have:

$$C_{ij}(\Delta P_{ij}) \propto \frac{1}{P_{surplus_i}} \quad (19)$$

$$C_{ij}(\Delta P_{ij}) \propto \frac{1}{\text{Number of nodes in control region of bus } i} \quad (20)$$

$$C_{ij}(\Delta P_{ij}) \propto P_{losses}(ij). \quad (21)$$

$Q_{losses}(ij)$ is the increment of technical losses due to the component of current related to increases in Q flow and is given by $R_{ij}(\frac{Q_{ij}^{t+12} - Q_{ij}^{t2}}{V_j^{t2}})$ [16]. Consequently, we derive $P_{losses}(ij)$ as:

$$P_{losses}(ij) = R_{ji}(\frac{P_{ij}^{t+12} - P_{ij}^{t2}}{V_j^{t2}}). \quad (22)$$

IV. PROBLEM FORMULATION

A. Control Strategy Based on Apparent Power (S) Modulation

HVAC units provide temperature trajectory information to the agent. The agent receives voltage magnitude and angle information from the smart meter. If the grid voltage profile goes out of its operational limits, the agent calculates the necessary amount of active and reactive power considering the reference values received from the grid, and selects the HVAC units that need to be controlled according the optimized temperature trajectories. The agent sends the control signal back to each DMPC and the control actions are applied. The agent makes the binary decision of ON/OFF based on its algorithm, as illustrated in Fig. 1.

On the other hand, each HVAC unit has a certain capacity in OFF condition. In case the required apparent power exceeds the capacity of the system, we assume it provides the maximum possible with the same requested angle.

The flow chart of determining apparent power via DMPC is shown in Fig. 2

B. Optimization

The problem of estimating the optimal contribution of active and reactive power from neighboring buses and the bus at which voltage regulation is desired is formulated as a cost minimization problem. $\beta = (i, j, \dots, n)$ is the set of all the busses on the region, and j is the bus at which voltage regulation is desired under the control region of β . The optimization cost function coordinates the amount of active and reactive power supplied from each of these buses to improve the voltage profile at bus i both in terms of magnitude and angle. Active and reactive power are coupled, so a constraint on apparent power must be defined.

By having active power, reactive power, and proportionality constants a_{ij} and b_{ij} , the loss minimization is defined as follows:

$$\min C_s(i) = \sum_{i \in \beta} a_{ij} P_{losses}(ij) + \sum_{i \in \beta} b_{ij} Q_{losses}(ij) \quad (23)$$

s.t.

$$S_{ij} = \sqrt{(P_{ij})^2 + (Q_{ij})^2} \quad (24)$$

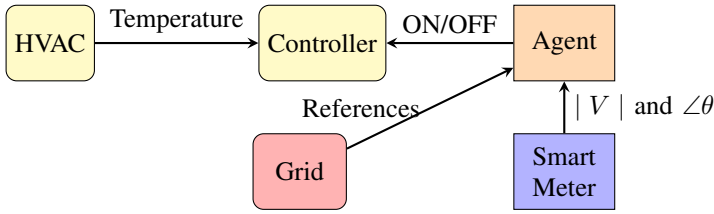


Fig. 1. Flowchart of decision making process of the agent

$$Q_{ij}^{t+1} \leq Q_{surplus_j} \quad \text{and} \quad P_{ij}^{t+1} \leq P_{surplus_j} \quad (25)$$

$P_{surplus_j}$ and $Q_{surplus_j}$ are obtained from priority slack and are sum of maximum active and reactive power each HVAC unit can provide. Equation (25) was defined so that the amount we receive do not exceed the required amount.

$$0.95pu \leq V_j^t + S_{v\Delta Q_{ij}} \Delta Q_j \leq 1.05pu \quad (26)$$

$$0.95pu \leq V_j^t + S_{v\Delta P_{ij}} \Delta P_j \leq 1.05pu \quad (27)$$

and

$$118.8^\circ \leq \theta_j^t + S_{\theta\Delta Q_{ij}} \Delta Q_j \leq 121.2^\circ \quad (28)$$

$$118.8^\circ \leq \theta_j^t + S_{\theta\Delta P_{ij}} \Delta P_j \leq 121.2^\circ \quad (29)$$

We assume $1 pu$ as the voltage magnitude reference and 120° as the angle reference. $\pm 5\%$ for magnitude and $\pm 1\%$ for angle tolerance range are considered.

Solving the aforementioned cost function will give us the optimal contribution of both active (P_{ji}) and reactive (Q_{ji}) power from bus i to improve both the voltage at bus j and the global frequency. With surplus active power at bus j ($P_{surplus_j}$) and surplus reactive power at bus j ($Q_{surplus_j}$) being known quantities, the agent determines the ON/OFF state of each HVAC unit according to the active and reactive power demand by having the knowledge of the optimal trajectory of HVAC units in its control region for the prediction horizon.

By considering providing power to the grid as positive injection and absorbing power as negative injection, the following conditions are possible:

- Positive reactive power injection for under voltage ($V < 0.95 pu$)
- Negative reactive power injection for over voltage ($V > 1.05 pu$)
- Positive active power injection for under frequency ($\theta < 118.8^\circ$)
- Negative active power injection for over frequency ($\theta > 121.2^\circ$)

For positive power injection, HVAC units which are about to turn OFF will be turned OFF, while for negative power injection, HVAC units which are about to turn ON will be turned ON to absorb power.

Frequency is related to the angle indirectly. Angle θ is defined as the difference between the voltage angle with

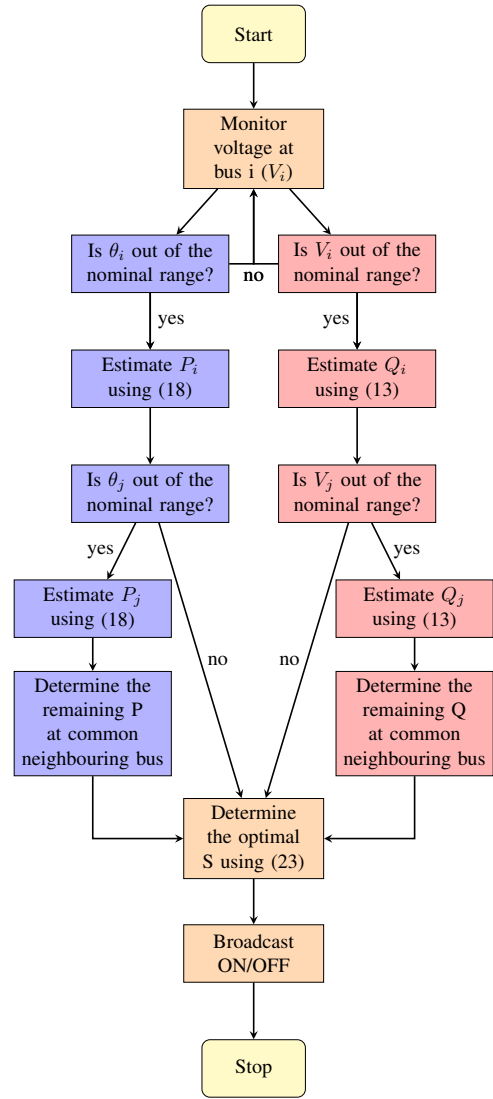


Fig. 2. DMPC flowchart for determining apparent power (S)

a reference that rotates always at $60Hz$. The power flow equations in (12) consider a constant frequency [1]. Instead of relying on the time domain equations, we make a quasi-static analysis by considering the correlation of the frequency with the angle change. Reference angle θ is assumed to be 120° for phase C and a $60Hz$ frequency reference. Local QoS is ensured by implementing the state space model which determines the appropriate control signal to maintain customer comfort by remaining within the temperature bounds set by the customer.

V. CASE STUDY

Test results are obtained considering the modified IEEE 13 Test Feeder System illustrated in Fig. 3 and modeled in MathWorks Simulink [17]. Besides removing capacitor banks at nodes 652 and 611 for testing the robustness of the DMPC control strategy on the voltage profile, a synchronous generator is used as the system source at node 650 for the frequency

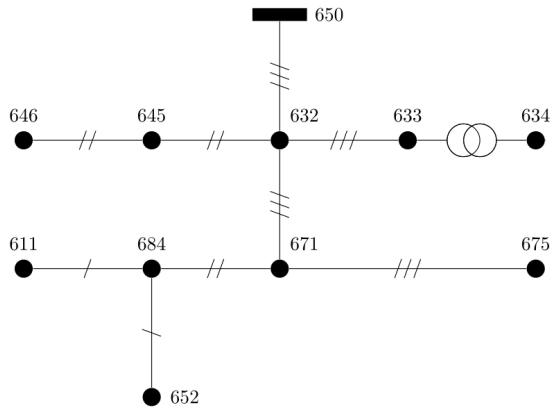


Fig. 3. 13 bus test system

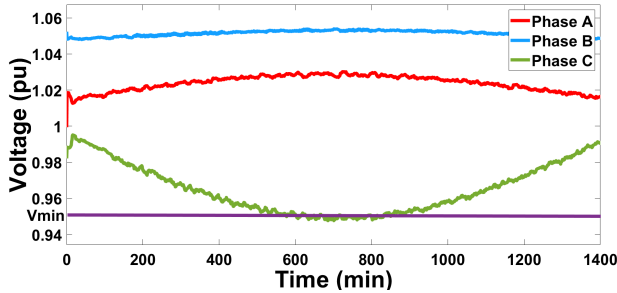


Fig. 4. Uncontrolled voltage profile

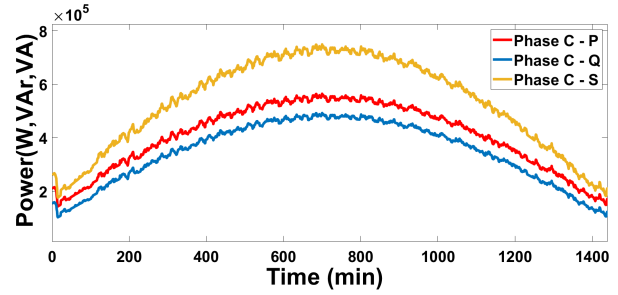


Fig. 5. Active, reactive and apparent power on node 675 without control

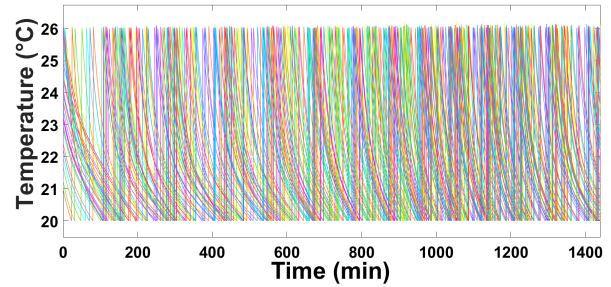


Fig. 6. Temperature trajectories of node 675 without control

regulation analysis. The nominal power of the synchronous generator is 6.5 kW with 3.7 inertia constant. A population of 40 homogeneous HVAC systems (with 5kW, 4kVAr rating) at each bus were considered in the simulation with a narrow temperature dead band of $3\text{ }^{\circ}\text{C}$ and a set point of 23°C for a cold day. Since the IEEE 13 Test Feeder System is a radial system and just neighbouring areas contribute to the node power, the results considering the optimization problem in (23) were not considered in the Simulink model.

Firstly, we demonstrate some of the system profiles without any control strategy applied. Bus 675 is chosen for analysis since it is at the end of the line and is more sensitive to violations. Fig. 4 and Fig. 5 show the voltage profile, active, reactive, and apparent power on node 675 while Fig. 6 illustrates the temperature trajectories when no control strategies are applied to the system. Fig. 7 also shows the frequency profile derived from the phase C voltage angle of bus 675. As can be seen in Fig. 4, the phase C voltage profile is below the lower bound of nominal range, and frequency in Fig. 7 is oscillating around 60 Hz .

Active, reactive, apparent power, and temperature trajectories of the system are shown in Fig. 9 and Fig. 10 for the node 675 when controlled on phase C for the 24°C set temperature.

Fig. 8 shows how voltage violation improves after applying the DMPC on phase C at node 657 of the system. In this case, the agent turns OFF HVAC units with the set temperature $> 24^{\circ}\text{C}$ at $t + 1$ to provide the necessary active and reactive

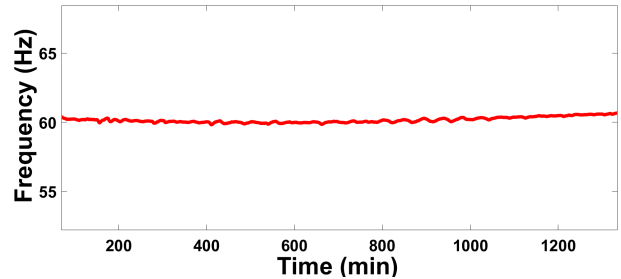


Fig. 7. Frequency monitored on node 675 without control

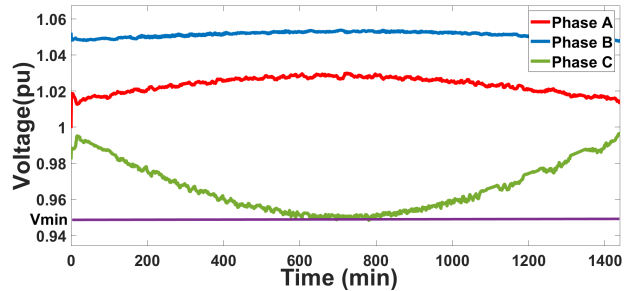


Fig. 8. Voltage profile at node 675 (24°C)

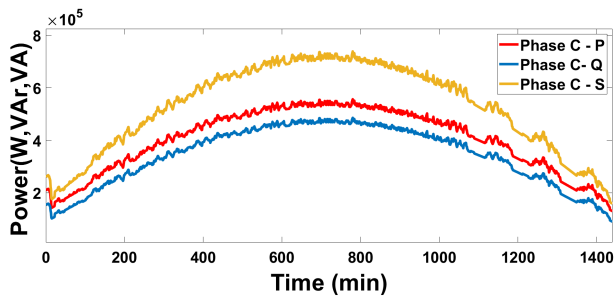


Fig. 9. Active, reactive and apparent power on node 675 using DMPC (24°C)

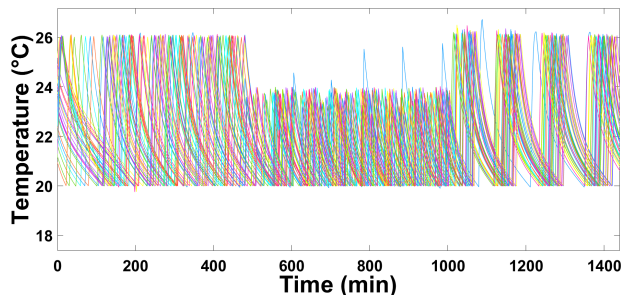


Fig. 10. Temperature trajectories of node 675 with control on (24°C)

power.

Finally, Fig. 11 illustrates the frequency profile when controlled by the DMPC strategy for control over 23°C , and control over 24°C , and the uncontrolled case. As can be seen in the inset between 850 min and 1050 min, the frequency oscillation improves with the DMPC strategy. The small changes in frequency are justified by the limited availability of the controlled HVAC loads.

VI. CONCLUSION

A DMPC strategy is presented to provide both active and reactive power support from smart buildings to attenuate power quality by optimizing a cost function related to the room temperature in smart buildings. Multiple simulations for different temperatures have been conducted and the comparison of different cases have been demonstrated. The feasibility of obtaining better voltage and frequency profiles by providing

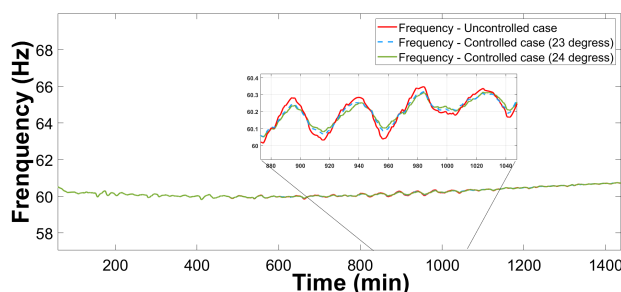


Fig. 11. Comparison of frequency monitored on node 675 between uncontrolled, controlled over 23°C and 24°C

both active and reactive power from DERs is explored and promising results are obtained.

Future work could focus on obtaining the algorithm of the agent which determines the exact apparent power with the angle. Additionally, testing the strategy for a more sophisticated system could be investigated.

REFERENCES

- [1] P. Kundur, "Power System Stability and Control," 2005.
- [2] X.B. Gu, Y.S. Wu, T. Qu, W. Xu and D.N. Liu, "The simulation of the controllable reactor and its application in Ultra High Voltage Transmission Lines", IEEE International Conf. Advanced Power System Automation and Protection (APAP), pp. 1833-1837, 2011.
- [3] M. Baran and F. F. Wu, "Optimal sizing of capacitors placed on a radial distribution system," in IEEE Transactions on Power Delivery, vol. 4, no. 1, pp. 735-743, Jan. 1989, doi: 10.1109/61.19266.
- [4] A. Moreno-Muñoz, Power quality: mitigation technologies in a distributed environment. Springer Science Business Media, 2007.
- [5] A. Molina-García, F. Bouffard and D. S. Kirschen, "Decentralized Demand-Side Contribution to Primary Frequency Control," in IEEE Transactions on Power Systems, vol. 26, no. 1, pp. 411-419, Feb. 2011, doi: 10.1109/TPWRS.2010.2048223.
- [6] Y. G. Rebours, D. S. Kirschen, M. Trotignon and S. Rossignol, "A Survey of Frequency and Voltage Control Ancillary Services—Part I: Technical Features," in IEEE Transactions on Power Systems, vol. 22, no. 1, pp. 350-357, Feb. 2007, doi: 10.1109/TPWRS.2006.888963.
- [7] N. Lu, "An Evaluation of the HVAC Load Potential for Providing Load Balancing Service," in IEEE Transactions on Smart Grid, vol. 3, no. 3, pp. 1263-1270, Sept. 2012, doi: 10.1109/TSG.2012.2183649.
- [8] H. Hao, B. M. Sanandaji, K. Poolla and T. L. Vincent, "Aggregate Flexibility of Thermostatically Controlled Loads," in IEEE Transactions on Power Systems, vol. 30, no. 1, pp. 189-198, Jan. 2015, doi: 10.1109/TPWRS.2014.2328865.
- [9] W. Zhang, J. Lian, C. Chang and K. Kalsi, "Aggregated Modeling and Control of Air Conditioning Loads for Demand Response," in IEEE Transactions on Power Systems, vol. 28, no. 4, pp. 4655-4664, Nov. 2013, doi: 10.1109/TPWRS.2013.2266121.
- [10] X. Wu, J. He, Y. Xu, J. Lu, N. Lu and X. Wang, "Hierarchical Control of Residential HVAC Units for Primary Frequency Regulation," in IEEE Transactions on Smart Grid, vol. 9, no. 4, pp. 3844-3856, July 2018, doi: 10.1109/TSG.2017.2766880.
- [11] Y. Lin, P. Barooah, S. Meyn and T. Middelkoop, "Experimental Evaluation of Frequency Regulation From Commercial Building HVAC Systems," in IEEE Transactions on Smart Grid, vol. 6, no. 2, pp. 776-783, March 2015, doi: 10.1109/TSG.2014.2381596.
- [12] S. C. Dhulipala, R. V. A. Monteiro, R. F. d. Silva Teixeira, C. Ruben, A. S. Bretas and G. C. Guimarães, "Distributed Model-Predictive Control Strategy for Distribution Network Volt/VAR Control: A Smart-Building-Based Approach," in IEEE Transactions on Industry Applications, vol. 55, no. 6, pp. 7041-7051, Nov.-Dec. 2019, doi: 10.1109/TIA.2019.2941179.
- [13] S. C. Dhulipala, C. Ruben, A. Bretas, R. V. A. Monteiro and G. C. Guimarães, "A Distributed Strategy for Volt/VAR Control in Distribution Networks: A Smart Buildings Approach," 2018 North American Power Symposium (NAPS), Fargo, ND, 2018, pp. 1-6, doi: 10.1109/NAPS.2018.8600660.
- [14] L. Wang, Control System Design and Implementation Using MATLAB. Springer Science and Business Media, 2008, vol 53, p. 287.
- [15] R. Aghatehrani and A. Golnas, "Reactive power control of photovoltaic systems based on the voltage sensitivity analysis," 2012 IEEE Power and Energy Society General Meeting, San Diego, CA, 2012, pp. 1-5, doi: 10.1109/PESGM.2012.6345477.
- [16] L. Mănescu and D. Ruşinaru, "Loss based performance index for the reactive power control," 2012 13th International Conference on Optimization of Electrical and Electronic Equipment (OPTIM), Brasov, 2012, pp. 307-312, doi: 10.1109/OPTIM.2012.6231932.
- [17] The Mathworks, Inc., Natick, Massachusetts, MATLAB version 10.1 (R2020a), Nov 2019.